ARTICLE

Synthesis of Hierarchically Porous $CaFe_2O_4$/Carbon Fiber Hybrids and Microwave Induced Catalytic Activity

Yi Song, Chao Kong, Jia Li*

School of Material Science and Engineering, University of Jinan, Jinan 250022, China

(Dated: Received on July 29, 2014; Accepted on December 22, 2014)

Hierarchically porous $CaFe_2O_4$/carbon fiber hybrids with enhanced microwave induced catalytic activity for the degradation of methyl violet (MV) from water were synthesized from kapok by a novel two-step process coupling pore-fabricating and nanoparticles assembling. The as-prepared samples exhibited characteristic hollow fiber morphology, $CaFe_2O_4$ nanoparticles dispersed uniformly on the surface of hollow carbon fibers (HCF). The effects of various factors such as $CaFe_2O_4$ loading, microwave power, catalyst doses, initial concentration of MV solution and pH value on the microwave induced degradation of MV over $CaFe_2O_4$/HCF were evaluated. It was found that the microwave induced degradation of MV over $CaFe_2O_4$/HCF had high reaction rate and short process time. The kinetic study indicated that the degradation of MV over $CaFe_2O_4$/HCF followed pseudo-first-order kinetics model. The high catalytic activity of $CaFe_2O_4$/HCF was facilitated by the synergistic relationship between microwave induced catalytic reaction and adsorption characteristics.

Key words: $CaFe_2O_4$, Microwave, Catalytic activity, Kapok, Degradation

I. INTRODUCTION

Large numbers of pigments and dyes are often used for industrial applications. There are approximately 10^4 various industrial pigments and dyes, and annual production of over 7×10^5 tons [1−3]. Consequently, it is inevitable that pigments and dyes will appear in wastewater and spill into the environment without being effectively treated. Though there is a very small amount of dye in water (10−20 mg/L), color of effluents is highly visible [4].

Some methods have been used for the removal of pollutants from wastewater, such as chemical oxidations, adsorption [5, 6], biological decoloration [7], ultrasonic degradation [8], photocatalytic degradation [9, 10] and the advanced oxidation process with photo-Fenton reaction [11]. In recent years, microwave induced catalytic degradation (MICD) technologies [12, 13] merge as a useful and effective method to mineralize organic pollutants into non-toxic substances [14]. Microwave can be applied alone [15], combined with oxidants, integrated with photochemical process and Fenton process, and coupled with microwave-absorbing materials. As known, some materials including porous carbon [16, 17], metal oxidation [18] and ferromagnetic materials [19, 20] are widely used as microwave-absorbing materials.

Hierarchically porous catalysts containing both interconnected macroporous and mesoporous structure exhibit enhanced catalytic activity due to combining the accessible mass transport pathway of macroporous tunnel with high surface area. A large variety of natural materials, such as bacteria [21], diatoms [22], butterfly wings [23] and egg membranes [24] have been used to synthesize hierarchically porous materials. Notably, the cellulose-based substance becomes major concern in synthesizing biomorphic materials due to its low cost, reproducibility and stable chemical composition mainly containing C and O.

In this work, hierarchically porous $CaFe_2O_4$/HCF hybrids were synthesized using kapok as biotemplate. The microwave-enhanced catalytic activity of $CaFe_2O_4$/HCF hybrids on the degradation of methyl violet (MV) was investigated. The influences of processing parameters on the resulting products, and the microstructure characteristic relating to catalytic activity were evaluated in detail.

II. EXPERIMENTS

A. Catalyst preparation and characterization

All the chemicals used in this study, such as $Ca(NO_3)_2{\cdot}6H_2O$, $Fe(NO_3)_3{\cdot}3H_2O$, hydrochloric acid, sodium hydroxide, and MV, were of analytical grade. Kapoks were purchased from the local market. After being pre-oxidation treated at 200 °C for 2 h, kapok was impregnated with aqueous solution of analytical

*Author to whom correspondence should be addressed. E-mail: mse_lij@ujn.edu.cn, Tel.: +86-13953185430

grade of iron nitrate and calcium nitrate aqueous mixture at room temperature, and then dried at 120 °C for 4 h, hydrolysis and condensation reactions occurred. The white hybrid material was then heated in a tube furnace at 800 °C for 1 h under a constant flow of N_2 at 0.2 L/min. The as-prepared samples were obtained with different $CaFe_2O_4$ loading on HCF of 0wt%, 5wt%, 10wt%, 15wt%, 20wt%, 100wt%, designated as $CaFe_2O_4$/HCF-0, $CaFe_2O_4$/HCF-5, $CaFe_2O_4$/HCF-10, $CaFe_2O_4$/HCF-15, $CaFe_2O_4$/HCF-20, $CaFe_2O_4$/HCF-100.

Scanning electron microscopy (SEM, FEI QUANTA FEG250, USA) were equiped with energy-dispersive X-ray spectrometry (EDS). The samples were identified by X-ray diffractometry (XRD, Huber diffractometer, Rimsting, Germany) pattern (Cu-Kα radiation source RUC300, λ=1.5418 Å, voltage 40 kV, current 160 mA, Rigaku, Japan). BET surface area was measured by nitrogen adsorption-desorption technique at 77 K using a physisorption analyzer (ASAP2020M+C, Micrometrics, GA, USA). Brunauer-Emmett-Teller and Barrett-Joyner-Halenda (BET/BJH) methods were used to determine specific surface area and porosity. pHS-3C pH meter (Shanghai Leici Company, China) was used to determine acidities of the MV solutions. The UV continuous spectrum was obtained by UVC3200 (Daojin, Japan). The magnetization measurements were carried out by MicroMag 2900 AGM (alternating gradient magnetometer, Princeton Measurements Corporation, USA).

B. Microwave assisted catalytic oxidation of MV

A 50 mL MV solution (5 mg/L) with pH close to 7.0 and a certain amount of catalyst were added in a beaker. The G8023ESL-V8 microwave oven (Guangdong Galanz Company, China) with microwave frequency of 2.45 GHz and output power of 800 W was used to irradiate this suspension for a certain time. Then the suspension was cooled for 5 min in the water bath and separated using a centrifuge. The UV-Vis absorption spectra of parathion solutions were recorded on Cary-50 UV-Vis spectrometer (Varian Company, USA). The absorbance was determined at the maximum absorbance wavelength (580 nm) of MV. Then degradation rate r was obtained by the following equation:

$$r = \frac{C_0 - C_t}{C_0} \times 100\% \tag{1}$$

where C_0 is the initial concentration of MV and C_t is the concentration of MV at time t.

III. RESULTS AND DISCUSSION

A. Characterization of $CaFe_2O_4$/HCF

The structure and components of the as-prepared $CaFe_2O_4$/HCF samples were characterized by XRD analysis. Figure 1 shows the typical XRD pattern of the as-prepared samples. The main characteristic diffraction peaks of $CaFe_2O_4$ (JCPDS card No.08-0100) were observed at 2θ values of approximately 19.1°, 25.4°, 33.6°, 35.6°, 40.4°, 42.8°, 49.8°, 55.3°, 60.6°, 61.4°, 72.0°, which could be assigned to (120), (220), (040), (201), (131), (311), (401), (260), (600), (161), (322) diffraction planes, respectively. It is worth noting that the diffraction baseline of XRD pattern was very broad, which could be attributed to the presence of amorphous carbon. Moreover, a small amount of $Ca_2Fe_2O_5$ (JCPDS card No.11-0675) was observed. The average crystallite size D of the $CaFe_2O_4$ grain was 4.6 nm calculated by the Scherrer equation:

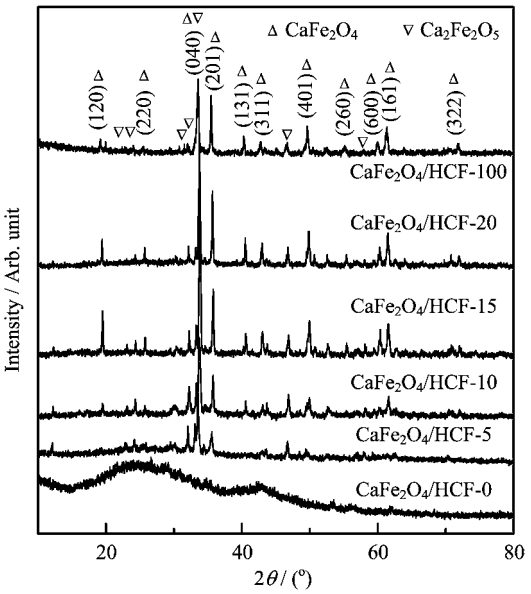

FIG. 1 XRD pattern of the as-prepared samples.

$$D = \frac{K\lambda}{\beta \cos\theta} \tag{2}$$

where K is a constant equal to 0.89, λ is the X-ray wavelength equal to 0.154 nm, β is the full width at half maxima of the most intense peak, and θ is the half diffraction angle.

Figure 2 (a) and (b) show the SEM images of raw kapok. It was found that raw kapok was characterized by the interwoven networks consisting of hollow fibers. The average diameter of hollow fibers was about 18 μm (Fig.2(b)). For the synthesized sample, the hollow fiber morphology of kapok was retained (Fig.2 (c)−(e)). The diameters of hollow tubes ranged from 10 μm to 15 μm which were smaller than those of raw kapok due to the shrinkage caused by high temperature treatment. Tiny particles were found on the surface of HCF (Fig.2(c)). As revealed in Fig.2(d), $CaFe_2O_4$ particles on the surface of HCF increased and distributed non-uniformly due to increasing concentration of iron nitrate solution and calcium nitrate solution. When the concentration

DOI:10.1063/1674-0068/28/cjcp1407125

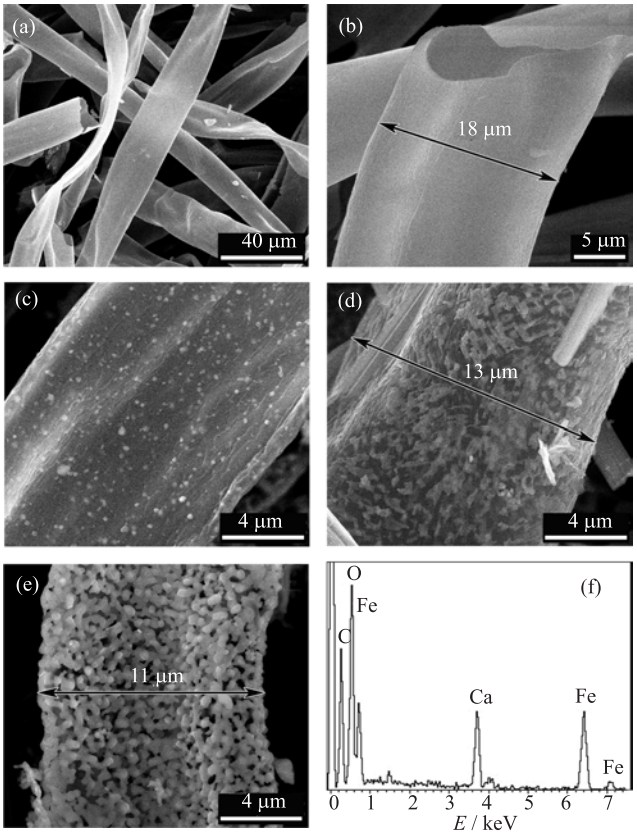

FIG. 2 SEM images of Kapok template (a, b) and $CAFE_2O_4$/HCF-10 (c, d, e). (f) EDS of $CAFE_2O_4$/HCF-10.

of iron nitrate solution and calcium nitrate solution increased again, carbon was almost burned as shown in Fig.2(e). The typical EDS of particles (Fig.2(f)) indicated that they were composed of Ca, Fe, and O. According to the above XRD result, we assumed that these particles were $CaFe_2O_4$ and $Ca_2Fe_2O_5$.

The nitrogen adsorption-desorption isotherm and corresponding pore size distributions of synthesized $CaFe_2O_4$/HCF-10 sample are shown in Fig.3. According to the IUPAC classification scheme, the isotherm (Fig.3(a)) belonged to the group of type IV, indicating that $CaFe_2O_4$/HCF was mesoporous material. The BET specific surface area, average pore size, and pore volume of the $CaFe_2O_4$/HCF were measured to be 85.49 m^2/g, 5.3 nm, and 0.114 cm^3/g, respectively.

As a promising technique for the recycling of the catalyst, magnetic separation could avoid the loss of catalyst. The magnetization measurements were carried out at room temperature in air. As shown in Fig.4, the hysteresis loops of the as-prepared $CaFe_2O_4$/HCF-10 catalyst indicated that it was the ferromagnetic material. The saturation magnetization (M_s) of the $CaFe_2O_4$/HCF-10 catalyst was calculated to be 16.92646 emu/g, which was enough to recover the catalyst from dye solution [25−27].

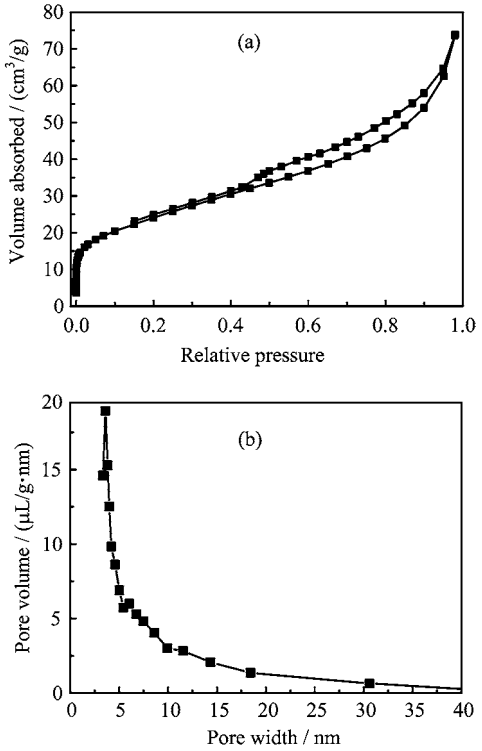

FIG. 3 (a) Nitrogen adsorption/desorption isotherms and (b) corresponding BJH pore diameter distribution of as-prepared $CaFe_2O_4$/HCF-10 sample.

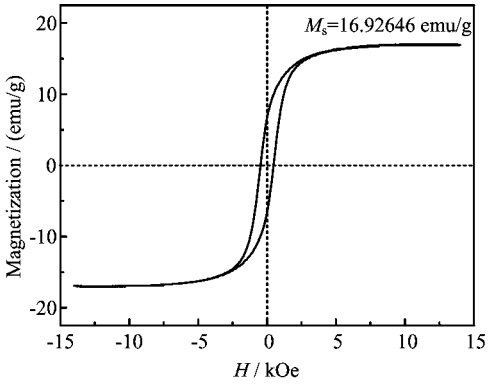

FIG. 4 Magnetic hysteresis loops of porous $CaFe_2O_4$/HCF-10 sample at room temperature.

B. Changes in the UV-Vis absorption spectrum of MV

The UV-Vis absorption spectra of MV at different microwave irradiation time (t) are shown in Fig.5. As could be seen from the spectra, before the treatment, the UV-Vis spectrum of MV was characterized by one main band in the visible region, with its maximum absorption at 580 nm, and two bands in the ultraviolet region located at 246 and 300 nm. The band at 246 nm was ascribed to the benzene ring in the dye molecule, and the bands at 300 and 580 nm were attributed to the absorption of chromophore containing NH_2 group.

DOI:10.1063/1674-0068/28/cjcp1407125

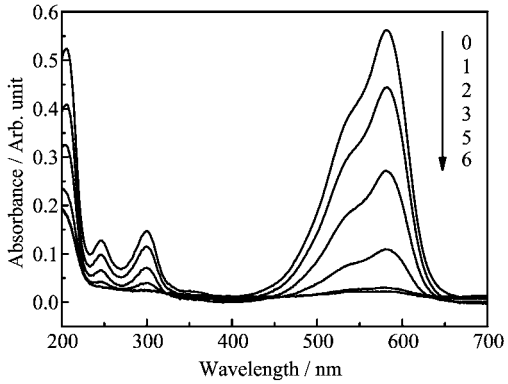

FIG. 5 UV-Vis absorption of Aldrich HA during microwave degradation at different time t (0−6 min).

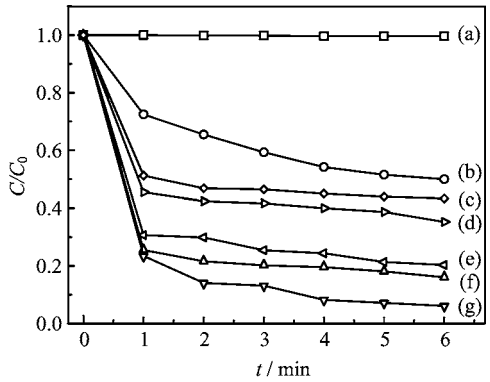

FIG. 6 Effect of $CaFe_2O_4$ loading on degradation of MV. (a) Without catalyst, (b) $CaFe_2O_4$/HCF-0, (c) $CaFe_2O_4$/HCF-100, (d) $CaFe_2O_4$/HCF-20, (e) $CaFe_2O_4$/HCF-15, (f) $CaFe_2O_4$/HCF-5, (g) $CaFe_2O_4$/HCF-10.

It was obvious that these bands steadily decreased with increasing t. When t was 6 min, all bands became flat, which indicated that the MV was completely mineralized.

C. Effect of loading on MV degradation

$CaFe_2O_4$ loading on HCF usually played an important role in decolorization process of MV. Figure 6 shows that degradation of MV hardly occurs in the absence of $CaFe_2O_4$/HCF under 800 W microwave irradiation. From Fig.6, it could be seen that the extent of degradation increased with increasing $CaFe_2O_4$ loading from 0wt% to 10wt%, and then degradation rate dropped to some extent at ratio of 10wt%−100% $CaFe_2O_4$. The optimum loading of $CaFe_2O_4$ considering degradation rate was 10%, because that the number of "hot spots" on the surface of $CaFe_2O_4$/HCF increased with increased catalyst loading, which could enhance oxidation of MV. When $CaFe_2O_4$ loading increased from 10wt% to 20wt%, catalyst surface area may be reduced owing to agglomeration of the particles

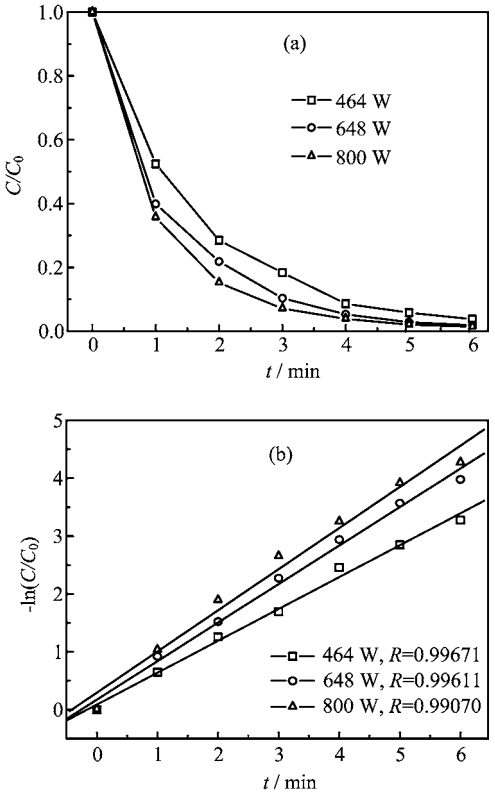

FIG. 7 Effect of microwave powers (a) and kinetics (b) on degradation rate of MV. 5 mg/L MV, 50 mL MV, 0.3 g/L $CaFe_2O_4$/HCF-10.

[28]. In addition, it could be seen that degradation rate of $CaFe_2O_4$/HCF was higher than that of HCF alone (49.99%) and $CaFe_2O_4$ alone (56.67%).

D. Effect of microwave power and initial concentration of MV on the degradation of MV

Three levels of microwave power were used to investigate the effect of microwave power on the degradation of MV (Fig.7). It was found that the removal ratio of MV increased and the decolorization process became faster with the microwave power increasing (Fig.7(a)), because that higher microwave power could form more "hot spots" on the surface of $CaFe_2O_4$/HCF and produce more ·OH radical in the aqueous solution. Hence, in subsequent experiments, 800 W was chosen because of the best degradation rate.

Pseudo first-order kinetic model [29] was used to investigate the effect of microwave power on the degradation of MV:

$$\ln\left(\frac{C_0}{C_t}\right) = k_{\text{app}}t \tag{3}$$

where C_0 is the initial concentration of MV, C_t is the concentration of MV at each t and k_{app} is the apparent rate constant. The $-\ln(C/C_0)$ versus t are plotted and

DOI:10.1063/1674-0068/28/cjcp1407125

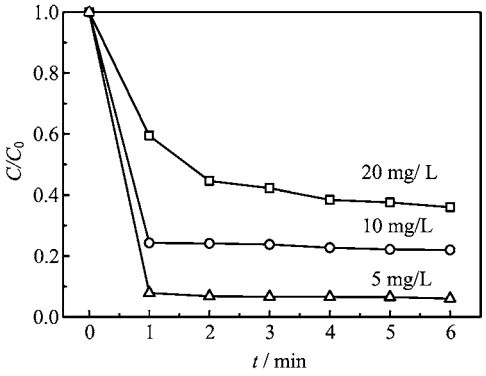

FIG. 8 Effects of and initial concentration on degradation rate. 50 mL MV, 0.3 g/L $CaFe_2O_4$/HCF-10, 800 W.

TABLE I Kinetic parameters from $-\ln(C/C_0)$ *vs.* t plots for different microwave powers.

Microwave power/W	k_{app}/min^{-1}	R^2
464	0.55118	0.99343
648	0.66596	0.99224
800	0.71152	0.98149

shown in Fig.7(b). It could be seen that the relationship between $-\ln(C/C_0)$ and t for each concentration was approximately linear. Table I shows the rate constants and linear correlation coefficients (R^2). The R^2 values obtained from pseudo-second-order model were close to unity, indicating that the degradation of MV fitted this model well. It is worth noting that the rate constant increased with increasing microwave powers. The highest rate constant was obtained as the microwave power was 800 W.

The effect of initial concentration of MV on the degradation of MV is shown in Fig.8. It could be seen that degradation rate of MV was the highest as the initial concentration of MV was 5 mg/L. This was because that the amount of MV molecules around the limited $CaFe_2O_4$/HCF catalyst increased with increasing dye concentration. In other words, the catalytic reactions were limited by the concentration of ·OH radicals. Hence, the degradation rate decreased with increasing C_0.

E. Effects of catalyst doses and pH on the degradation of MV

The effect of catalyst doses on the degradation of MV was investigated under microwave power 800 W. As shown in Fig.9(a), the degradation rate of MV increased with increasing catalyst dose. The degradation rate of three catalyst doses (5, 10, and 15 mg) were 65.2%, 88%, and 96%, respectively when t was 6 min. The experiments demonstrated that degradation rate of MV increased with increasing catalyst dose. This

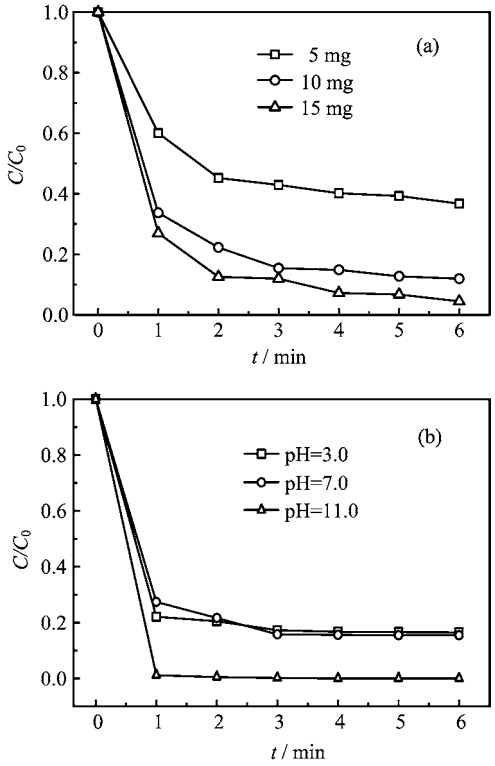

FIG. 9 Effects of catalyst doses (a) and pH (b) on degradation rate. 50 mL MV, 0.3 g/L $CaFe_2O_4$/HCF-10, 800 W.

was due to the fact that the number of "hot spots" on the surface of $CaFe_2O_4$/HCF increased with increase of catalyst doses under microwave irradiation. In addition, the increasing $CaFe_2O_4$/HCF could produce more ·OH radicals. All of factors show clearly the increase of degradation capacity of $CaFe_2O_4$/HCF with catalyst doses rising.

The initial pH value was one of the most important parameter on decolorization process because the wastewater containing dye usually had a wide range of pH values. The change of pH could influence the surface charge of $CaFe_2O_4$/HCF sample, and thus affected the reaction speed of degradation in the end. It could be seen from Fig.9(b) that the degradation rates of MV at pH=3, 7, and 11 were 83.5%, 84.5%, and 100%, respectively after 6 min microwave radiation. The $CaFe_2O_4$/HCF sample had the highest degradation rate at pH=11.0, which indicated that the degradation of MV was more effective in alkaline conditions. The effect of pH value might be explained from the viewpoint of adsorption. MV was readily to be adsorbed through π-π stacking and ionic interaction due to the fact that MV was an alkaline and cationic triphenylmethane dyes [30]. In the acidic conditions (pH<4.0), the positively charged surface of catalyst resulted in repulsion between $CaFe_2O_4$/HCF and MV, so the adsorption occurred only through the π-π stacking which led to a lower degradation efficiency. With the pH increas-

DOI:10.1063/1674-0068/28/cjcp1407125

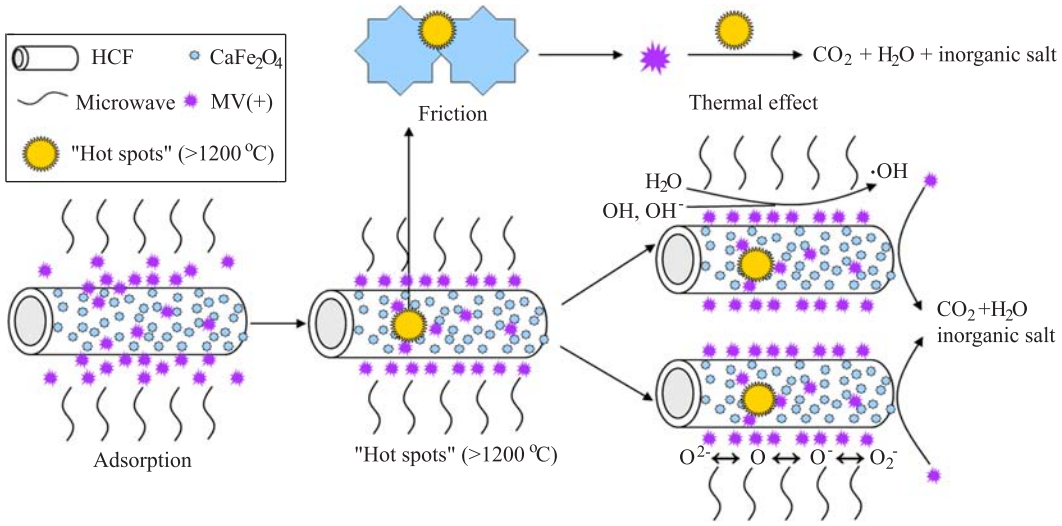

FIG. 10 Illustration of degradation of MV on the surface of $CaFe_2O_4$/HCF.

ing, the increasing negative charges were beneficial to the interaction between $CaFe_2O_4$/HCF and cationic dye MV. In addition, the production of ·OH radicals needed the alkaline conditions (pH>7.0), which assisted in the MICD. Based on the above reasons, $CaFe_2O_4$/HCF exhibited higher catalytic activity at pH=11.0.

F. Possible degradation mechanism

Although the investigation on the microwave degradation in the presence of $CaFe_2O_4$/carbon fibers hybrids has not been reported too much yet, three ways to degrade MV may be deduced based on our studies (Fig.10). First, the microwave irradiation can induce a rotation and a migration violently for the motion of polar molecules in $CaFe_2O_4$/HCF as microwave absorbent under microwave irradiation, leading to a fast increase of the solution temperature due to friction. Also, with increasing of collision numbers between polar molecules, the violent motion of polar substances can transform microwave energy into the "hot spots" that would reach over 1200 °C [31]. Then, not only the chromophore containing NH_2 group of MV can be degraded rapidly but also the benzene ring of it can be destroyed completely due to the function of thermal effect. Second, H_2O, OH^-, and OH groups in the structure of $CaFe_2O_4$ can be transformed into ·OH in aqueous solution due to such high temperature, which can non-selectively attack organic contaminants [32] and convert them into H_2O, CO_2, and inorganic salt. The existence of ·OH results in accelerating the degradation rate of MV. In addition, there is synergy between $CaFe_2O_4$ and microwave. Due to such high temperature, the electrophilic oxygen ions (O^{2-}, O^- and O_2^-) that come from the lattice oxygen on $CaFe_2O_4$ ferrite show high catalytic activity in MICD and can be donated to participate in the degradation of MV [33, 34]. In this work, there may be one or more mechanisms of degradation. Therefore, the as-prepared $CaFe_2O_4$/HCF may be considered to be good catalyst in MICD.

IV. CONCLUSION

In this work, the biomorphic $CaFe_2O_4$/HCF with high microwave induced catalytic activity for degradation of MV was prepared by using kapok as template. Hierarchically porous $CaFe_2O_4$/HCF hybrid catalysts exhibited hollow carbon fibers loaded with $CaFe_2O_4$ nanoparticles. The catalytic performances of synthesized samples for the degradation of MV under microwave irradiation were investigated. It was demonstrated that the degradation process of MV over $CaFe_2O_4$/HCF catalyst was a fast process. Under the conditions of 50 mg/L and 50 mL MV solution, 0.3 g/L catalyst dose and microwave power 800 W, completely degradation of MV could be obtained after 6 min microwave irradiation. The microwave induced degradation of MV fitted pseudo first-order kinetic model.

V. ACKNOWLEDGMENTS

This work was supported by the National Natural Science Foundation of China (No.51172095 and No.61102006).

[1] E. Y. Ozmen, M. Sezgin, A. Yilmaz, and M. Yilmaz, Bioresour. Technol. **99**, 526 (2008).
[2] M. Chivukula, J. T. Spadaro, and V. Renganathan, Biochemistry **34**, 7765 (1995).

DOI:10.1063/1674-0068/28/cjcp1407125

[3] C. I. Pearce, J. R. Lloyd, and J. T. Guthrie, Dyes Pigments **58**, 179 (2003).
[4] K. T. Chung and S. E. Stevens, Environ. Toxicol. Chem. **12**, 2121 (1993).
[5] L. S. Zhang, J. S. Lian, L. X. Wang, J. Jiang, Z. R. Duan, and L. J. Zhao, Chem. Eng. J. **241**, 384 (2014).
[6] K. Mohanty, J. T. Naidu, B. C. Meikap, and M. N. Biswas, Ind. Eng. Chem. Res. **45**, 5165 (2006).
[7] J. J. Jones and J. O. Falkinham, Antimicrob. Agents Chemother. **47**, 2323 (2003).
[8] E. Villaroel, J. Silva-Agredo, C. Petrier, G. Taborda, and R. A. Torres-Palma, Ultrason. Sonochem. **21**, 1763 (2014).
[9] L. J. Deng, Y. Z. Gu, W. X. Xu, and Z. Y. Ma, Chin. J. Chem. Phys. **27**, 321 (2014).
[10] C. Li and W. D. Wang, Chin. J. Chem. Phys. **22**, 423 (2009).
[11] R. Colombo, T. C. R. Ferreira, S. A. Alves, R. L. Carneiro, and M. R. V. Lanza, J. Environ. Manage. **118**, 32 (2013).
[12] K. C. Li, R. G. Xing, S. Liu, Y. K. Qin, X. T. Meng, and P. C. Li, Int. J. Biol. Macromol. **51**, 767 (2012).
[13] N. Remya and J. G. Lin, Chem. Eng. J. **166**, 797 (2011).
[14] P. Klan and M. Vavrik, J. Photochem. Photobiol. **177**, 24 (2006).
[15] G. Cravotto, A. Binello, S. Di Carlo, L. Orio, Z. L. Wu, and B. Ondruschka, Environ. Sci. Pollut. Res. **17**, 674 (2010).
[16] L. L. Bo, X. Quan, S. Chen, H. M. Zhao, and Y. Z. Zhao, Water. Res. **40**, 3061 (2006).
[17] G. S. Zhang, J. H. Qu, H. J. Liu, A. T. Cooper, and R. C. Wu, Chemosphere **68**, 1058 (2007).
[18] T. L. Lai, C. C. Lee, G. L. Huang, Y. Y. Shu, and C. B. Wang, Appl. Catal. B **78**, 151 (2008).
[19] L. Zhang, M. M. Su, and X. J. Guo, Sep. Purif. Technol. **62**, 458 (2008).
[20] L. Zhang, X. J. Guo, F. Yan, M. M. Su, and Y. Li, Water Sci. Technol. **60**, 2563 (2009).
[21] H. Zhou, T. X. Fan, and D. Zhang, Chem. Mater. **19**, 2144 (2007).
[22] N. L. Rosi, C. S. Thaxton, and C. A. Mirkin, Angew. Chem. Int. Ed. **43**, 5500 (2004).
[23] J. Y. Huang, X. D. Wang, and Z. L. Wang, Nano. Lett. **6**, 2325 (2006).
[24] D. Yang, L. Qi, and J. Ma, Adv. Mater. **14**, 1543 (2002).
[25] Y. M. Ren, Q. Dong, J. Feng, J. Ma, Q. Wen, and M. L. Zhang, J. Colloid. Interface. Sci. **382**, 90 (2012).
[26] M. Shahid, J. L. Liu, Z. Ali, I. Shakir, M. F. Warsi, R. Parveen, and M. Nadeem, Mater. Chem. Phys. **139**, 566 (2013).
[27] A. A. Farghali, M. H. Khedr, and A. F. Moustafa, Mater. Technol. **23**, 104 (2008).
[28] M. P. Titus, V. Garcöa-Molina, M. A. Banos, J. Gimenez, and S. Esplugas, Appl. Catal. B **47**, 219 (2004).
[29] Z. H. Zhang, J. Jiatieli, D. N. Liu, F. Y. Yu, S. Xue, W. Gao, Y. Y. Li, and D. D. Dionysiou, Chem. Eng. J. **231**, 84 (2013).
[30] C. Z. Li, Y. H. Dong, J. J. Yang, Y. Y. Li, and C. C. Huang, J. Mol. Liq. **196**, 348 (2014).
[31] H. M. Kingston and L. B. Jassie, *Introduction to Microwave Sample Preparation*, Washington: American Chemical Society, (1998).
[32] J. Wang, W. Sun, Z. H. Zhang, Z. Jiang, X. F. Wang, R. Xu, R. H. Li, and X. D. Zhang, J. Colloid Interface Sci. **320**, 202 (2008).
[33] T. L. Lai, Y. L. Lai, and C. C. Lee, Catal. Today. **131**, 105 (2008).
[34] A. Bielański and J. Haber, Catal. Rev. Sci. Eng. **19**, 1 (1979).

DOI:10.1063/1674-0068/28/cjcp1407125